RESEARCH PAPER

Self-Similar Solution of Radial Stagnation Point Flow and Heat Transfer of a Viscous, Compressible Fluid Impinging on a Rotating Cylinder

Asghar B. Rahimi[1] · Hamid Mohammadiun[2] · Mohammad Mohammadiun[2]

Abstract

In this study, the radial stagnation point flow of strain rate $\bar{k}$ impinging on a cylinder rotating at constant angular velocity ω and its heat transfer are investigated. Reduction in the Navier–Stokes equations and energy equation to primary nonlinear ordinary differential equation systems is obtained by use of appropriate transformations when the angular velocity and wall temperature or wall heat flux all are constant. The impinging free stream is steady and normal to the surface from all sides, and the range of Reynolds number variation ($Re = \bar{k}a^2/2\upsilon$) is 0.1–1000 in which a and υ are cylinder radius and kinematic viscosity, respectively. Flow results are presented for selected values of compressibility factor and different values of Prandtl numbers along with shear stress and Nusselt number. For all values of Reynolds numbers and surface temperature or surface heat flux, as compressibility factor increases the radial velocity field, the heat transfer coefficient and the wall shear stress increase, whereas the angular velocity field decreases. The rotating movement of the cylinder does not have any effect on the radial component of the velocity, but its increase increases the angular component of the fluid velocity field and the surface shear stress.

Keywords Stagnation point flow · Constant angular velocity · Heat transfer · Compressibility factor · Constant wall temperature and heat flux

List of symbols

a	Cylinder radius
$c(\eta)$	Density ratio
$f(\eta)$	Function of η
$G(\eta)$	Function of η
k	Thermal conductivity
$\bar{k}$	Free stream strain rate
p	Fluid pressure
P	Non-dimensional pressure
Pr	Prandtl number
q_{w}	Heat flux at the wall
r, ϕ, z	Cylindrical coordinates
$Re = \frac{\bar{k}a^2}{2\upsilon}$	Reynolds number
T	Temperature
T_{w}	Wall temperature
T_{∞}	Free stream temperature
u	Radial component of the velocity
v	Angular component of the velocity
w	Axial component of the velocity
Nu	Nusselt number

Greek symbols

β	Compressibility factor
$\Gamma(\eta)$	Function related to density
η	Similarity variable
$\theta(\eta)$	Non-dimensional temperature
μ	Viscosity
υ	Kinematic viscosity
ω	Angular velocity of the cylinder
$\rho(\eta)$	Fluid density
ρ_{∞}	Free stream density
σ	Shear stress
ψ	Stream function
$\hat{\psi} = \frac{\psi}{0.5ka^3}$	Normalized stream function

✉ Hamid Mohammadiun
   hmohammadiun@iau-shahrood.ac.ir

1. Faculty of Engineering, Ferdowsi University of Mashhad, P.O. Box 91775-1111, Mashhad, Iran

2. Department of Mechanical Engineering, Shahrood Branch, Islamic Azad University, Shahrood, Iran

🌳 Shiraz University   ⚛ Springer

1 Introduction

Rotating movement of a cylinder in the case of stagnation point flow and heat transfer has many applications in manufacturing processes. For example, cooling or cleaning processes of punching instruments and drilling tools are samples of the industrial applications. The following picture may best describe how a radial flow can be arranged in order to coat the surface of a cylinder with any kind of protection material which is another application. This coating can be considered as protection against erosion or for the purpose of insulation. The flow on the cylinder comes from all directions (Fig. 1).

Existing solutions of the problem of axisymmetric stagnation point flow and heat transfer on either a cylinder or a flat plate are for viscous, incompressible fluid. The classical two-dimensional Hiemenz (1911) and three-dimensional Homann (1936) stagnation flows describe situations where fluid impinges normally onto a flat surface and spreads out bidirectionally or radially along the surface, away from a single stagnation point. The analogous problems have been solved by Howarth (1951) and Davey (1951) whose results for stagnation flow against a flat plate for asymmetric cases were presented. Wang (1973, 1974) was the first one who reported the solution for steady radial stagnation flow impinging on a stationary cylinder with impermeable walls, and this was continued by Gorla's works (1976, 1977, 1978a, 1978b, 1979) which are a series of steady and unsteady flows and heat transfer over a circular cylinder in the vicinity of the stagnation point for the cases of constant axial movement and the special case of axial harmonic motion of a non-rotating cylinder. Cunning et al. (1998) have investigated the nature of axisymmetric radial stagnation flow on a rotating circular cylinder with constant angular velocity, but their research is reliable in the case of incompressible fluid. Grosch and Salwen (1982) as well as Takhar et al. (1999) studied special cases of unsteady viscous flow on an infinite circular cylinder. The most recent works of the same types are the ones by Saleh and Rahimi (2004) and Rahimi and Saleh (2007, 2008), which are exact solution studies of a stagnation point flow and heat transfer on a circular cylinder with time-dependent axial and rotational movements, as well as studies by Abbasi and Rahimi (2009, 2009, 2012; Abbasi et al. 2011) which are exact solutions of stagnation point flow and heat transfer but on a flat plate. The mixed convection flow over a continuous moving vertical slender cylinder under the combined buoyancy effect of thermal and mass diffusion was studied by Takhar et al. (2000, 2002), and in the next study, the laminar natural convection boundary layer flow on an isothermal vertical thin cylinder embedded in thermally stratified high porosity medium was considered by them. Flow of two immiscible fluids in porous and non-porous channels was studied by Chamkha (2000) in which the steady laminar hydromagnetic flow and heat transfer of two immiscible fluids in vertical channel fitted with a uniform porous medium were considered. Takhar et al. (2001) presented the similarity solution of unsteady three-dimensional MHD-boundary
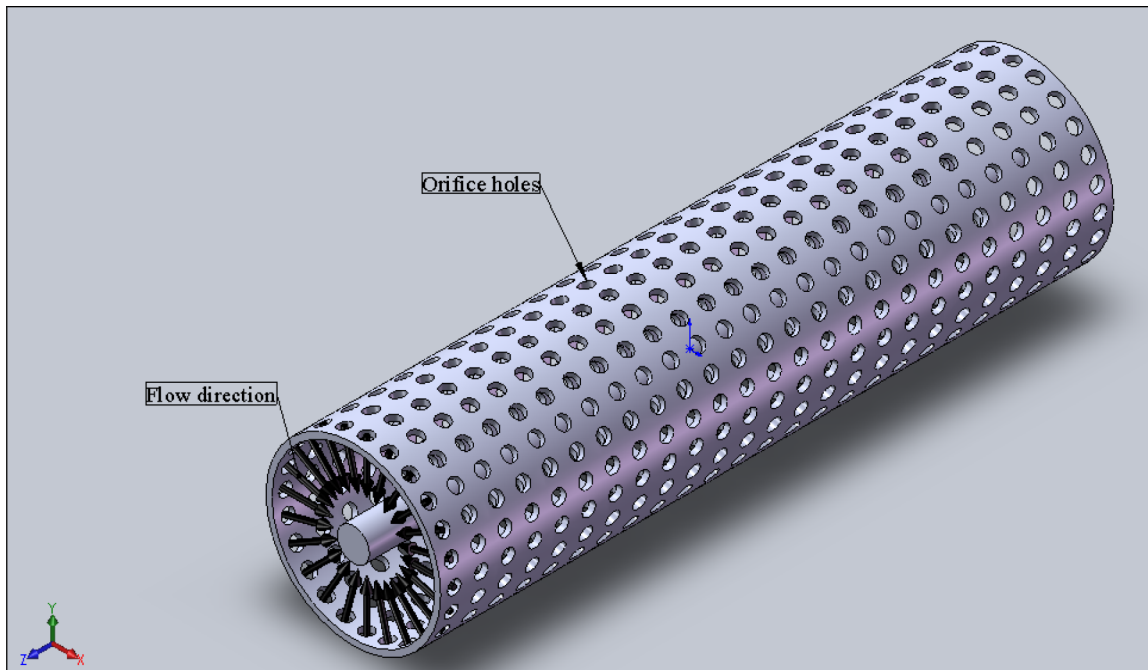
Fig. 1 A schematic mechanism of the radially impinging flow production

layer flow due to the impulsive motion of a stretching surface. In their paper, the effects of stretching and magnetic parameters on surface shear stress and surface heat transfer were reported. An exact solution for the steady laminar magnetohydrodynamic (MHD) thermosolutal Marangoni convection in the presence of a uniform applied magnetic field was presented by Magyari and Chamkha (2008) in which they obtained exact analytical solutions for the velocity, temperature and concentration boundary layers when the surface tension varies linearly with both the temperature and concentration and where the interface temperature and concentration are quadratic functions of the interface arc length. Mudhaf and Chamkha (2005) solved the problem of Marangoni flow over a flat surface due to imposed temperature and concentration gradients. They assumed that the surface tension varies linearly with temperature and concentration, but the wall temperature and concentration variations are quadratic functions of the location. Chamkha and Khaled (2000) investigated the problem of coupled heat and mass transfer by mixed convection in a linearly stratified stagnation flow (Hiemenz flow). The objective of their research was to consider simultaneous heat and mass transfer of an electrically conducting fluid by mixed convection in a stagnation flow over a flat plate embedded in a porous medium in the presence of fluid wall blowing or suction, magnetic field effects and temperature-dependent heat generation or absorption effects. Similarity solution for unsteady MHD flow near a stagnation point of a three-dimensional porous body with heat and mass transfer, heat generation/absorption and chemical reaction was presented by Chamkha and Ahmed (2011). They transformed the governing equations into a self-similar form and solved the extracted ordinary differential equation systems by tri-diagonal implicit finite difference method. Umavathi and Chamkha (2005) could obtain temperature and velocity distributions for the problem of unsteady oscillatory flow and heat transfer of two viscous immiscible fluids through a horizontal channel with time-dependent oscillatory wall transpiration velocity. They extracted exact solution for momentum and energy equation in their research.

Some existing compressible flow studies but in the stagnation region of bodies and by using boundary layer equations include the study by Subhashini and Nath (1999) as well as Kumari and Nath (1980, 1981) which are in the stagnation region of a body and also work by Katz (1972) as well as Afzal and Ahmad (1975), Libby (1967) and Gersten et al. (1978) which are all general studies in the stagnation region of a body. The only study that deals with stagnation point flow and heat transfer of a viscous, compressible fluid on a cylinder is by Mohammadiun and Rahimi (2012; Mohammadiun et al. 2013; Rahimi et al. 2016). They obtained an exact solution of the Navier–

Stokes equations for the case of a stationary cylinder. In their previous studies, Mohammadiun and Rahimi considered the stationary cylinder where the momentum equations are solved only in z and r directions.

The problem of stagnation point flow and heat transfer for the case of compressible fluid when the cylinder is rotating has not been considered so far. In this research work, solution of the problem of axisymmetric stagnation point flow and heat transfer is presented for the case of compressible, viscous fluid on a rotating cylinder when its angular velocity is constant. In the present analysis, because of rotational movement of the cylinder, in addition to the momentum equations in z and r directions the momentum equation in φ direction is also solved. An accurate numerical solution of the Navier–Stokes equations and the energy equation is obtained. The self-similar solution is reached by introducing the appropriate similarity variables. Sample distributions of shear stress and temperature fields at Reynolds numbers ranging from 0.1 to 1000 are presented for different values of Prandtl numbers and fluid compressibility factor.

2 Problem Formulation

The problem of laminar steady axisymmetric stagnation point flow and heat transfer of a viscous compressible fluid on a circular cylinder is aimed to be solved when the cylinder is rotating at a constant angular velocity. In order to solve this problem, the cylindrical coordinate system (r, φ, z) with associated unit vectors $(\hat{e}_r, \hat{e}_\varphi, \hat{e}_z)$ and corresponding velocity components (u, v, w) are selected, as it is illustrated in Fig. 2. An external axisymmetric radial stagnation flow of strain rate $\bar{k} = \frac{U}{a}$ impinges on the cylinder of radius a, centered at $r = 0$, and U is radial
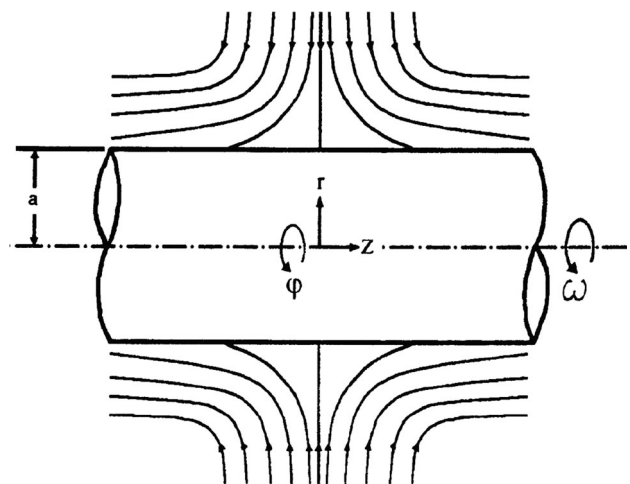

Fig. 2 Schematic diagram of a rotating cylinder

velocity injected from the outer cylinder toward the inner cylinder (Hong and Wang 2009). The steady Navier–Stokes and energy equations governing this problem are as follows.

Mass:

$$\frac{\partial(\rho u)}{\partial r} + \frac{\rho u}{r} + \frac{\partial(\rho w)}{\partial z} = 0 \tag{1}$$

r-momentum:

$$u\frac{\partial(\rho u)}{\partial r} - \frac{\rho v^2}{r} + w\frac{\partial(\rho u)}{\partial z} = -\frac{\partial P}{\partial r} + \upsilon\left\{\frac{1}{r}\frac{\partial}{\partial r}\left[r\frac{\partial(\rho u)}{\partial r}\right] - \frac{(\rho u)}{r^2} + \frac{\partial^2(\rho u)}{\partial z^2}\right\} \tag{2}$$

φ-momentum:

$$u\frac{\partial(\rho v)}{\partial r} + \frac{\rho uv}{r} + w\frac{\partial(\rho v)}{\partial z} = \upsilon\left\{\frac{1}{r}\frac{\partial}{\partial r}\left[r\frac{\partial(\rho v)}{\partial r}\right] - \frac{(\rho v)}{r^2} + \frac{\partial^2(\rho v)}{\partial z^2}\right\} \tag{3}$$

z-momentum:

$$u\frac{\partial(\rho w)}{\partial r} + w\frac{\partial(\rho w)}{\partial z}$$
$$= -\frac{\partial P}{\partial z} + \upsilon\left\{\frac{1}{r}\frac{\partial}{\partial r}\left[r\frac{\partial(\rho w)}{\partial r}\right] + \frac{\partial^2(\rho w)}{\partial z^2}\right\} \tag{4}$$

And energy,

$$\rho u\frac{\partial T}{\partial r} + \rho w\frac{\partial T}{\partial z} = \frac{\mu}{Pr}\frac{1}{r}\frac{\partial}{\partial r}\left(r\frac{\partial T}{\partial r}\right) \tag{5}$$

where p, ρ, υ and T are the fluid pressure, density, kinematic viscosity and temperature inside the boundary layer and after the impingement has occurred, respectively. The boundary conditions for velocity field are (Cunning et al. 1998):

$$r = a: \quad u = 0 \quad w = 0 \quad v = a\omega \tag{6}$$

$$r \to \infty: \quad u = -\bar{k}(r - a^2/r) \quad w = 2\bar{k}z \quad \lim_{r\to\infty}(rv) = 0 \tag{7}$$

in which (6) is no-slip conditions on the cylinder wall and ω is the angular velocity of the cylinder. To introduce the boundary conditions at large r, it must be referred to solution of the inviscid flow at the far distance from the cylinder which is obtained by considering Figure 3 and by using the continuity equation as follows.

$$r \to \infty : \frac{\partial(\rho U)}{\partial r} + \frac{\rho U}{r} + \frac{\partial(\rho w)}{\partial z} = 0,$$
$$(\rho = \rho_\infty) \Rightarrow \frac{\partial U}{\partial r} + \frac{U}{r} + \frac{\partial w}{\partial z} = 0 \tag{8}$$
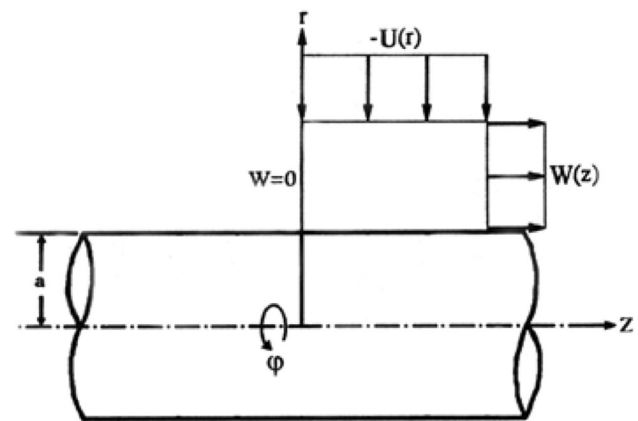$$\Rightarrow \frac{1}{r}\frac{\partial}{\partial r}(rU) + \frac{\partial w}{\partial z} = 0$$

Fig. 3 Schematic diagram of inviscid flow on cylinder

Transferring the term $\frac{\partial w}{\partial z}$ to the other side of the equation and considering that $\frac{1}{r}\frac{\partial}{\partial r}(rU)$ is the only function of r and $\frac{\partial w}{\partial z}$ is the only function of z, then this equality will exit only if it equals a constant value. According to the above explanations, the following results are obtained:

$$-\frac{1}{r}\frac{\partial}{\partial r}(rU) = \frac{\partial w}{\partial z} = C_1 = 2\bar{k} \tag{9}$$

In the above equation, $\bar{k}$ is strain rate of the stagnation point flow. By integrating Eq. (9), it gives:

$$U(r) = -\bar{k}r + \frac{C_2}{r} \tag{10}$$

Using the boundary condition, $r = a \to U = 0$, leads to $C_2 = \bar{k}a^2$ and the final form of $U(r)$ is presented by:

$$U(r) = -\bar{k}(r - a^2/r)$$

Relation (7) shows that the viscous flow solution approaches, in a manner analogous to the Hiemenz flow, the potential flow solution as $r \to \infty$ (Cunning et al. 1998).

For the temperature field, we have:

$$r = a: \begin{cases} T = T_w = \text{constant} & \text{for defined wall temperature} \\ \frac{\partial T}{\partial r} = -\frac{q_w}{k} & \text{for defined wall heat flux} \end{cases}$$
$$r \to \infty: \quad T \to T_\infty \tag{11}$$

where k is the thermal conductivity of the fluid and T_w and q_w are temperature and heat flux at the cylinder wall, respectively, and T_∞ is the free stream temperature.

A reduction in the Navier–Stokes equations is obtained by the following coordinate separation of the velocity field, which is actually modeled by the form of their limits as represented by Eq. (7). Also, a density ratio is introduced to indicate the change in density normal to the surface,

which gives back the similarity parameters for the case of an incompressible fluid:

$$u = -\frac{\bar{k}a^2}{r}\frac{\rho_\infty}{\rho(\eta)}f(\eta) \quad w = \frac{\rho_\infty}{\rho(\eta)}[2\bar{k}cf'(\eta)z]$$
$$v = +\frac{\bar{k}a^2}{r}\frac{\rho_\infty}{\rho(\eta)}G(\eta) \quad p = \rho_\infty\bar{k}^2a^2P \tag{12}$$

where

$$\eta = \frac{2}{a^2}\int_a^r\frac{\rho r}{\rho_\infty}\mathrm{d}r \tag{13}$$

is the dimensionless radial variable (Mohammadiun and Rahimi 2012) and prime denotes differentiation with respect to η and ρ_∞ is the free stream density. Note that, for the case of incompressible flow $[\rho(\eta) = \text{constant}]$, this variable is similar to the one in Wang (1974) except that it changes from zero to infinity instead of one to infinity. Transformations (12) satisfy (1) automatically, and their insertion into Eqs. (2), (3) and (4) yields a coupled system of differential equations in terms of $f(\eta), G(\eta)$ and an expression for the pressure:

$$\Gamma\left[c^3f''' + 3c^2c'f'' + c^2c''f' + (c')^2cf'\right] + c^2f'' + cc'f'$$
$$+ Re\left[1 + c'ff' + cff'' - c(f')^2\right] = 0 \tag{14}$$

$$\Gamma(c^2G'' + cc'G') + Re\,fG' = 0 \tag{15}$$

$$p - p_0 = \int_0^\eta\left[\frac{1}{2}\left(\frac{f}{\Gamma c}\right)^2 - \frac{ff'}{\Gamma c^2} + \frac{1}{2}\left(\frac{G}{\Gamma c}\right)^2 - \frac{1}{Re}(cf')'\right]$$
$$\mathrm{d}\eta - 2\left(\frac{z}{a}\right)^2 \tag{16}$$

In these equations, $c(\eta) = \frac{\rho(\eta)}{\rho_\infty}$, $Re = \frac{\bar{k}a^2}{2v}$, $\Gamma(\eta) = 1 + \int_0^\eta\frac{\mathrm{d}\eta}{c(\eta)}$ and prime indicates differentiation with respect to η. From conditions (6) and (7), the boundary conditions for (14) and (15) are as follows:

$$\eta = 0: \quad f = 0 \quad f' = 0 \quad G = \frac{a^2}{2v}\frac{\omega c(0)}{Re} \tag{17}$$
$$\eta \to \infty: \quad f' = 1 \quad G = 0$$

To model the variation of density with respect to temperature, the following Boussinesq approximation is used assuming low Mach number flow:

$$\rho \approx \rho_\infty\left[1 - \beta(T - T_\infty) - \frac{\beta^2}{2}(T - T_\infty)^2 - \frac{\beta^3}{3!}(T - T_\infty)^3\right]$$
$$\Rightarrow \rho/\rho_\infty = c(\eta) = 1 - \beta(T - T_\infty) - \frac{\beta^2}{2}(T - T_\infty)^2$$
$$- \frac{\beta^3}{3!}(T - T_\infty)^3 \tag{18}$$

in which β is compressibility factor.

To transform the energy equation into a non-dimensional form, we introduce:

$$\theta(\eta) = \begin{cases} \dfrac{T(\eta) - T_\infty}{T_w - T_\infty}, & \text{for the case of defined wall temperature} \\ \dfrac{T(\eta) - T_\infty}{\frac{aq_w}{2k}} = \dfrac{T(\eta) - T_\infty}{\gamma}, & \text{for the case of defined wall heat flux} \end{cases} \tag{19}$$

Making use of (12) and (19), the energy equation may be written as:

$$\frac{1}{Re \cdot Pr}\left[\Gamma\left(c^2\theta'' + cc'\theta'\right) + c\theta'\right] + f\theta' = 0 \tag{20}$$

with boundary conditions as:

$$\eta = 0:$$
$$\begin{cases} \theta = 1 & \text{for the case of defined wall temperature} \\ -\theta'\left[1 - \beta\gamma\theta - \frac{\beta^2}{2}\gamma^2\theta^2 - \frac{\beta^3}{3!}\gamma^3\theta^3\right] = 1 & \text{for the case of defined wall heat flux} \end{cases}$$
$$\eta \to \infty: \theta = 0 \quad \text{for both cases} \tag{21}$$

The local heat transfer coefficient is given by:

$$h = \begin{cases} \dfrac{q_w}{T_w - T_\infty} = -\dfrac{2k}{a}\theta'(0)c(0) & \text{for the case of defined wall temperature} \\ \dfrac{2k}{a}\dfrac{1}{\theta(0)} & \text{for the case of defined heat flux} \end{cases} \tag{22}$$

or in terms of Nusselt number:

$$Nu = \frac{ha}{2k}$$
$$= \begin{cases} -\theta'(0)c(0) & \text{for the case of defined wall temperature} \\ \dfrac{1}{\theta(0)} & \text{for the case of defined heat flux} \end{cases} \tag{23}$$

Because of $c(\eta)$, Eqs. (14), (15) and (20) depend on each other. Note that, for the case of incompressible fluid $\rho(\eta) = \rho_\infty$ and Eq. (14) is exactly reduced to the equation obtained in Wang (1974) for radial component of velocity and also Eq. (20) reduces to the equation obtained in Gorla (1976), with consideration of starting value for the variable η.

3 Shear Stress

The shear stress at the cylinder surface is obtained from:

$$\sigma = \sigma_\varphi \hat{e}_\varphi + \sigma_z \hat{e}_z = \mu \left[r \frac{\partial}{\partial r} \left(\frac{v}{r} \right) \hat{e}_\varphi + \frac{\partial w}{\partial r} \hat{e}_z \right]_{r=a} \quad (24)$$

But

$$\begin{cases} \dfrac{\partial w}{\partial r} = \dfrac{\partial w}{\partial \eta} \dfrac{\partial \eta}{\partial r} = [2\bar{k} f''(\eta) z] \dfrac{2r}{a^2} c(\eta) \\[2mm] r \dfrac{\partial}{\partial r} \left(\dfrac{v}{r} \right) = -\dfrac{2\bar{k} a^2}{r^2} \dfrac{G(\eta)}{c(\eta)} + 2\bar{k} \left[G'(\eta) - \dfrac{G(\eta) c'(\eta)}{c(\eta)} \right] \end{cases} \quad (25)$$

Since $\eta = 0$ at $r = a$, then we have

$$\begin{cases} \sigma_\phi = 2\mu\omega \left\{ -[1 + c'(0)] + \dfrac{\bar{k} G'(0)}{\omega} \right\} \\[2mm] \sigma_z = \dfrac{4\mu\bar{k}}{a} z f''(0) c(0) \end{cases} \quad (26)$$

Results of $\left| \frac{\sigma_\phi}{2\mu\omega} \right|$ for different values of Re numbers with Pr number held constant are presented in later sections.

As the governing equations show, considering compressibility effect causes the momentum equations and the energy equation to be coupled together which helps the designer to control the velocity gradient on the surface by varying this compressibility factor which eventually affects the surface tension.

4 Numerical Procedures

A finite difference procedure consisting of tri-diagonal matrix algorithm (*TDMA*) is used to numerically solve the governing Eqs. (14), (15) and (20) describing the sets of laws. The discrete form of the governing equations is a system of equations that is *tri-diagonal*. This special case of a system of quasi-linear equations has nonzero elements only on the diagonal plus or minus one column. Also, these couple equation systems are *band diagonal*, with nonzero elements only along a few diagonal lines adjacent to the main diagonal (above and below). The procedure of *LU* decomposition where L is the lower triangular (has elements only on the diagonal and below) and U is the upper triangular (has elements only on the diagonal and above), forward and backward substitution has been employed to solve the tri-diagonal sets (Press et al. 1997). The numerical procedure is repeated until the difference between the results of two repeated sequences of each of the equations becomes less than 0.00001.

To investigate the independency of the grid size, we used various step sizes. The results are reported in Table 1 for $Re = 100$, $Pr = 0.7$, $T_w = 400$ K and $\beta = 0.0033$. As

Table 1 Effect of step size on dimensionless functions, $\frac{2vRe}{a^2\omega} G(0.2)$ and $\theta(0.2)$

$\Delta\eta$	$\frac{2vRe}{a^2\omega} G(0.2)$	$\theta(0.2)$
0.005	0.05425	0.12133
0.003	0.05387	0.11824
0.001	0.05276	0.11679
0.0005	0.05271	0.11673

it can be seen, the value of the step size does not have significant effect on the dimensionless functions, $\frac{2vRe}{a^2\omega} G(0.2)$ and $\theta(0.2)$. Finally, uniform step size value ($\Delta\eta = 0.001$) is used to discrete the ordinary differential equations.

5 Validation of Numerical Procedures

Comparison of the normalized stream function $\hat{\psi} = \frac{\psi}{0.5 k a^3} = 2f(\eta)\left(\frac{z}{a}\right)$ with the results from Hong and Wang (2009) is shown in Fig. 15. All of the results have been extracted for the case of incompressible fluid ($\beta = 0$). In each case, there is a good conformity between the presented results and the results from Hong and Wang (2009).

6 Results and Discussions

In this section, the solution of the self-similar Eq. (15) along with surface shear stresses and Nusselt number for prescribed values of surface temperature and heat flux for selected values of Reynolds and Prandtl numbers are presented. Equations (14) and (20) are the same as in Mohammadiun and Rahimi (2012) which is for a stationary cylinder. Therefore, rotation of the cylinder does not have any effect on the radial component of the velocity and also the heat transfer.

As mentioned previously, stagnation point flow can be used in cleaning of drills and different cutting tools, for example. In this application, effect of the surface tension plays a great role since removing the unwanted materials from tools surface has a direct relationship on its increase. The presented results show how the increase in compressibility of the fluid produces a greater surface tension and also how the increase in the surface temperature or heat flux helps in removing the excess materials easily.
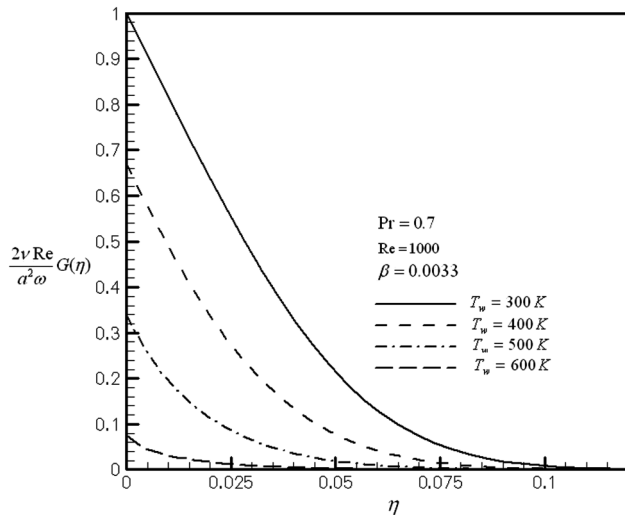
Effects of the surface temperature of the cylinder on the $\frac{2vRe}{a^2\omega} G(\eta)$ function for $\beta = 0.0033$, $Pr = 0.7$ and specified values of the Reynolds number are shown in Figs. 4 and 5. As surface temperature increases, the depth of the diffusion of these functions decreases which means that the angular component of the fluid velocity field for a specified angular velocity of the cylinder decreases as the surface
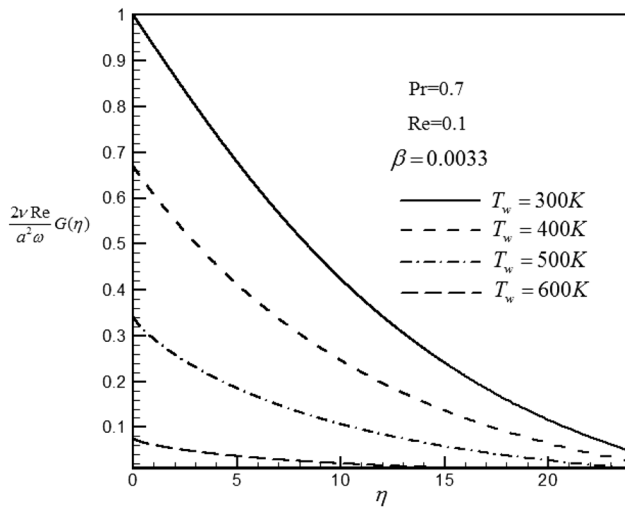
Fig. 4 Variation of $\frac{2\upsilon Re}{a^2\omega}G(\eta)$ in terms of η at $Re = 0.1$, $Pr = 0.7$ and $\beta = 0.0033$, for different values of wall temperatures
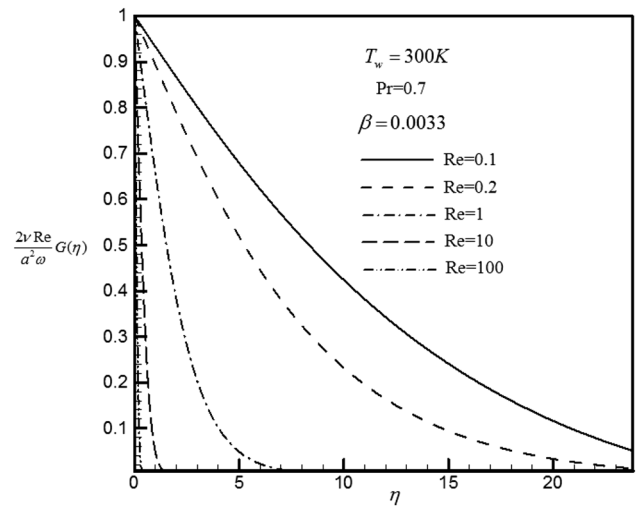
Fig. 6 Variation of $\frac{2\upsilon Re}{a^2\omega}G(\eta)$ in terms of η at $T_w = 300$ K, $Pr = 0.7$ and $\beta = 0.0033$, for different values of Reynolds numbers

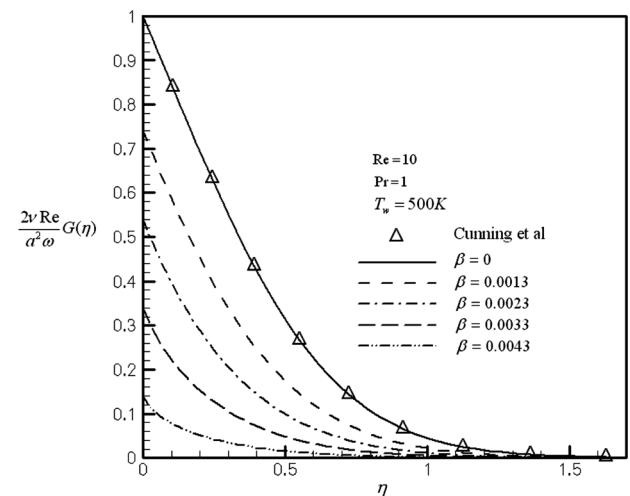The effect of change in the compressibility factor on the dimensionless function $\frac{2\upsilon Re}{a^2\omega}G(\eta)$ against η for $T_w = 500$ K, $Pr = 1$ and selected values of Reynolds number is depicted in Fig. 7. For each value of the Reynolds number, as compressibility factor increases, the depth of the diffusion of this function decreases which means that the angular component of the fluid velocity field for a specified angular velocity of the cylinder decreases as compressibility factor increases and also this decrease is larger when the cylinder rotates faster. It is worth mentioning that in each case incompressible fluid produces the largest amount of change in angular component of the fluid velocity field. In each case, the case of $\beta = 0$ is compared with the results of Cunning et al. (1998), which shows a perfect match. Same

Fig. 5 Variation of $\frac{2\upsilon Re}{a^2\omega}G(\eta)$ in terms of η at $Re = 1000$, $Pr = 0.7$ and $\beta = 0.0033$, for different values of wall temperatures

temperature increases and also this decrease is larger when cylinder rotates faster. This is because at a specific Reynolds number the increase in temperature which brings about a decrease in $c(\eta)$ would increase $\bar{k}/\mu$ meaning the radial inertial forces and brings about an increase in radial component of the velocity field and this phenomenon would decrease the angular component of the velocity field.

Sample profiles of the dimensionless function $\frac{2\upsilon Re}{a^2\omega}G(\eta)$ against η for the case of constant surface temperature for compressibility factor $\beta = 0.0033$, $Pr = 0.7$, $T_w = 300$ K and for selected values of Reynolds numbers are depicted in Fig. 6. As Reynolds number increases, the depth of the diffusion of this function decreases which means that the angular component of the fluid velocity field decreases.
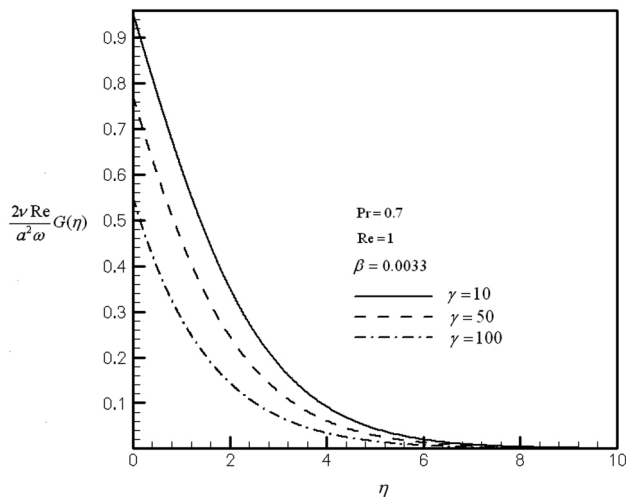

Fig. 7 Variation of $\frac{2\upsilon Re}{a^2\omega}G(\eta)$ in terms of η at $T_w = 500$ K, $Pr = 1$ and $Re = 10$, for different values of compressibility factor
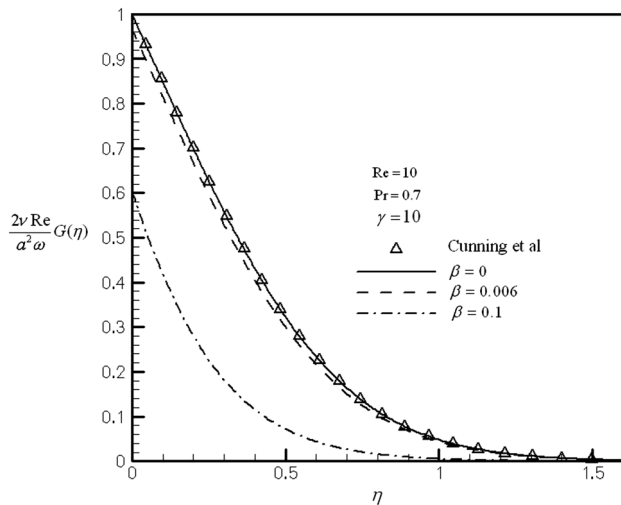
Fig. 8 Variation of $\frac{2\nu Re}{a^2 \omega} G(\eta)$ in terms of η at $\gamma = 10$, $Pr = 0.7$ and $Re = 10$, for different values of compressibility factor
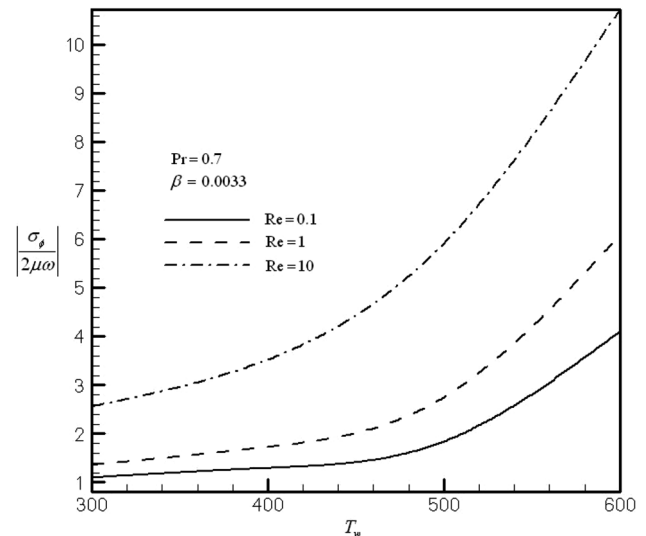

Fig. 9 Variation of $\frac{2\nu Re}{a^2 \omega} G(\eta)$ in terms of η at $\beta = 0.0033$, $Pr = 0.7$ and $Re = 1$, for different values of surface heat flux

Fig. 10 Variation of shear stress in terms of T_w at $Pr = 0.7$, $\beta = 0.0033$ for different values of Reynolds numbers

increasing the cylinder surface temperature from $T_w = 300$ K to $T_w = 400$ K the absolute value of the stress tensor for $Re = 250, 500, 750, 1000$ would increase by 35, 30.76, 37.45, 32.45%, respectively. This increase for $T_w = 500$ K and at the same values of Reynolds numbers is 82, 76.92, 85.7 and 91%, respectively. Also, since the increase in surface heat flux is in the same direction of the surface temperature, it would increase the stress tensor as much as 14.7 and 8.4% for $Re = 1, 10$, respectively, when it changes from $\frac{aq_w}{2k} = 1$ to $\frac{aq_w}{2k} = 50$.

Sample profiles of the local heat transfer coefficient (Nusselt number) against Reynolds number for the case of constant surface temperature and constant surface heat flux

type of information can be gathered from Fig. 8 but for a specified cylinder surface heat flux.

Figure 9 shows that as the surface heat flux increases the depth of the diffusion of $\frac{2\nu Re}{a^2 \omega} G(\eta)$ function decreases which is the same result as for the surface temperature case.
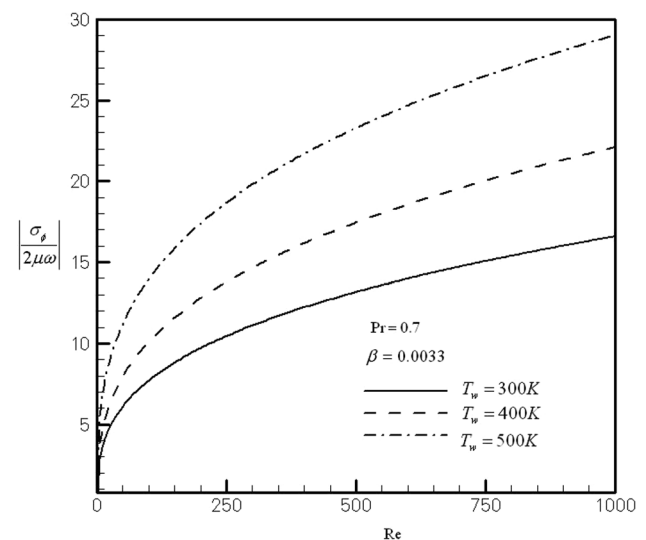
Change in shear stress versus the wall temperature is shown in Fig. 10 for selected values of Reynolds numbers. As it can be seen from this figure, the absolute value of the shear stress increases with the increase in Reynolds number or the wall temperature or the cylinder rotational speed. The same fact can be extracted from Fig. 11. Results with the same trend are depicted in Fig. 12 but for surface heat flux instead of surface temperature. For all these situations, the incompressible fluid case produces the least amount of shear stress. It can be deduced from these figures that by

Fig. 11 Variation of shear stress in terms of Reynolds number at $Pr = 0.7$, $\beta = 0.0033$ for different values of wall temperatures
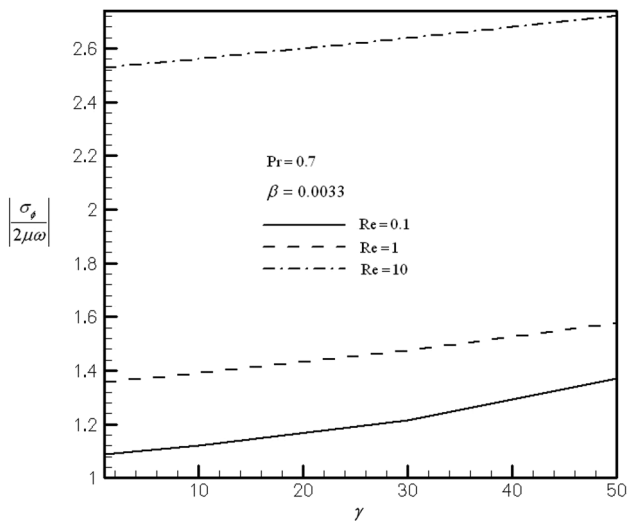
Fig. 12 Variation of shear stress in terms of wall heat flux at $Pr = 0.7$, $\beta = 0.0033$ for different values of Reynolds numbers

Fig. 14 Variation of Nusselt number in terms of Reynolds number at $Pr = 0.7$, $T_w = 500$ K for different values of compressibility factor

for compressibility factor $\beta = 0.0033$, $Pr = 0.7$ and for selected values of T_w and γ are presented in Fig. 13. As it can be seen from these figures, Nusselt number decreases by increase in the wall temperature or wall heat flux which means that the local heat transfer coefficient decreases. On the contrary, as Reynolds number increases the local heat transfer coefficient increases. Sample profiles of variation of Nusselt number in terms of Reynolds number at $Pr = 0.7$, $T_w = 500$ K and for different values of compressibility factor are presented in Fig. 14. As compressibility factor increases, the Nusselt number decreases. It is worth mentioning that the incompressible fluid produces the largest amount of convection heat transfer. It can be
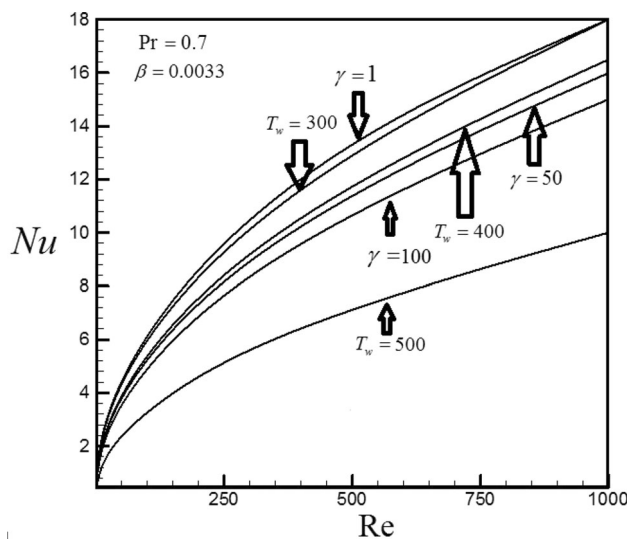

Fig. 13 Variation of Nusselt number in terms of Reynolds number at $Pr = 0.7$, $\beta = 0.0033$ for different values of wall temperatures or wall heat flux
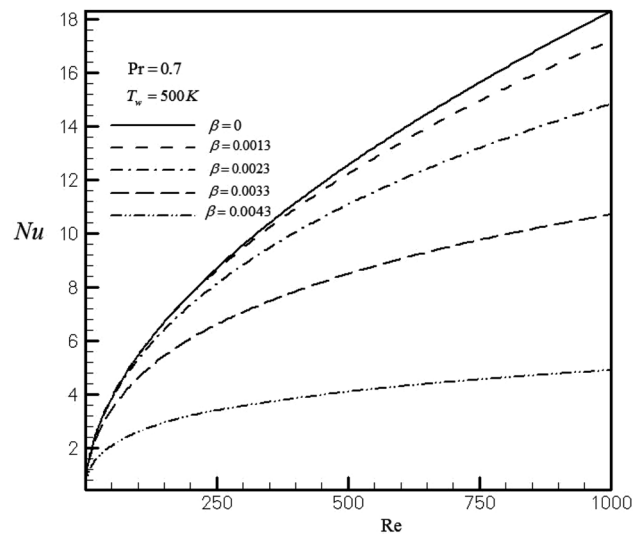
deduced from these figures that increase in cylinder surface temperature from $T_w = 300$ K to $T_w = 400$ K would decrease Nusselt number for $Re = 250$, 500, 750 and 1000 as much as 8.3, 6.7, 6 and 11.1%, respectively. This decrease for $T_w = 500$ K at the same Reynolds numbers is 50, 46.6, 43 and 46%, respectively. Increase in surface heat flux from $\frac{aq_w}{2k} = 1$ to $\frac{aq_w}{2k} = 50$ for the same values of Reynolds numbers would show 3.26, 14.7, 13.85 and 12.95% decrease in Nusselt number, respectively. This reduction for $\frac{aq_w}{2k} = 100$ is 21.74, 23.53, 22.9 and 22.28%. Also, increasing the fluid compressibility coefficient β from 0.0013, 0.0023, 0.0033 and 0.0044 would decrease Nusselt number by 9.4, 15.62, 39.06 and 68.75% for Reynolds number at 500.

An accurate numerical solution of the Navier–Stokes equations and energy equation has been derived for the steady-state viscous, compressible flow and heat transfer in the vicinity of an axisymmetric stagnation point of a rotating cylinder with a constant angular velocity. A reduction in these equations has been obtained by using appropriate transformations. The general self-similar solution has been obtained when the wall temperature of the cylinder or its wall heat flux is constant. All of the aforementioned solutions have been presented for Reynolds numbers $Re = \bar{k}a^2/2\upsilon$ ranging from 0.1 to 1000, selected values of compressibility factor and different values of Prandtl numbers. Shear stress and Nusselt number have been presented as well. Rotation of the cylinder does not have any effect on radial component of the velocity and also the heat transfer, but the angular component of the fluid velocity field increases as the angular velocity of the cylinder increases. The angular component of the fluid velocity field for a specified angular velocity of
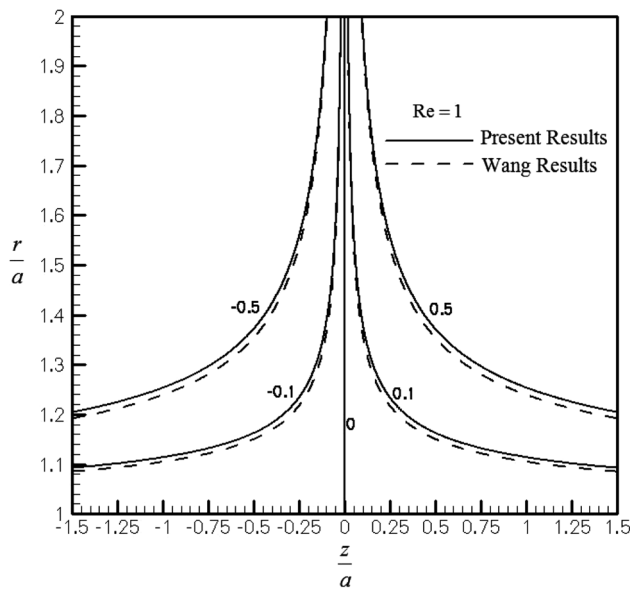
Fig. 15 Normalized stream function $\hat{\psi} = \frac{\psi}{0.5\bar{k}a^3} = 2f(\eta)\left(\frac{z}{a}\right)$ with, $Re = 1$. Fluid is injected from the outer cylinder at $\eta = 2$ toward the inner cylinder

the cylinder decreases as Reynolds number or compressibility factor or surface temperature or surface heat flux increases and this decrease in all cases is larger when the cylinder moves faster. It is worth mentioning that in each case the incompressible fluid produces the largest amount of change in angular component of the fluid velocity field. On the contrary, the angular component of the fluid velocity field increases as Prandtl number increases. Also, cylinder angular speed increases the absolute value of the shear stress and the amount of this shear stress is the least for the case of incompressible fluid. For the case of incompressible fluid, $\rho = \rho_\infty$ or $c(\eta) = 1$, and similarity variables and angular component of the velocity by Cunning et al. (1998), as well as energy equation by Gorla (1976), are obtained.

7 Conclusions

- Rotation of the cylinder does not have any effect on the radial component of the velocity and also the heat transfer.
- Increasing the cylinder surface temperature or surface heat flux would increase the surface stress tensor.
- Increasing the cylinder surface temperature or surface heat flux would decrease local Nusselt number.
- Angular component of the fluid velocity field increases as the angular velocity of the cylinder increases.
- The angular component of the fluid velocity field for a specified angular velocity of the cylinder decreases as

the Reynolds number or compressibility factor or surface temperature or surface heat flux increases and this decrease in all cases is larger when the cylinder moves faster.
- The angular component of the fluid velocity field increases as Prandtl number increases.

Appendix

Details of derivation of Eqs. (11), (12), (13) and (17) are presented as follows:

$$\eta = \frac{2}{a^2}\int_a^r \frac{\rho r}{\rho_\infty}\,\mathrm{d}r \Rightarrow \frac{\mathrm{d}\eta}{\mathrm{d}r} = \frac{2\rho r}{a^2\rho_\infty} \rightarrow \frac{\mathrm{d}\eta}{\mathrm{d}r} = \frac{2r}{a^2}c(\eta) \rightarrow 2r\mathrm{d}r$$

$$= a^2\frac{\mathrm{d}\eta}{c(\eta)} \longrightarrow \int\int_a^r 2r\mathrm{d}r = a^2\int_0^\eta \frac{\mathrm{d}\eta}{c(\eta)} \rightarrow r^2 - a^2$$

$$= a^2\int_0^\eta \frac{\mathrm{d}\eta}{c(\eta)} \rightarrow r^2 = a^2\left[1 + \int_0^\eta \frac{\mathrm{d}\eta}{c(\eta)}\right]$$

With definition: $\Gamma(\eta) = \left[1 + \int_0^\eta \frac{\mathrm{d}\eta}{c(\eta)}\right]$, we have: $r^2 = a^2\Gamma(\eta)$.

1. To derive pressure:

By use of non-dimensional pressure as:

$$p = \frac{P}{\rho_\infty \bar{k}^2 a^2} \Rightarrow P = \rho_\infty \bar{k}^2 a^2 p$$

Start from r-momentum:

$$u\frac{\partial(\rho u)}{\partial r} - \frac{\rho v^2}{r} + w\frac{\partial(\rho u)}{\partial z}$$
$$= -\frac{\partial P}{\partial r} + v\left\{\frac{1}{r}\frac{\partial}{\partial r}\left[r\frac{\partial(\rho u)}{\partial r}\right] - \frac{(\rho u)}{r^2} + \frac{\partial^2(\rho u)}{\partial z^2}\right\}$$

But:

$$\rho u = -\frac{\bar{k}a^2}{r}\rho_\infty f(\eta) \Rightarrow \frac{\partial(\rho u)}{\partial r} = \frac{\bar{k}a^2}{r^2}\rho_\infty f - 2\bar{k}\rho_\infty cf' \Rightarrow r\frac{\partial(\rho u)}{\partial r}$$
$$= \frac{\bar{k}a^2}{r}\rho_\infty f - 2\bar{k}\rho_\infty cf'r \Rightarrow \frac{\partial}{\partial r}\left[r\frac{\partial(\rho u)}{\partial r}\right]$$
$$= -\frac{\bar{k}a^2}{r^2}\rho_\infty f + \frac{\bar{k}a^2}{r}\rho_\infty f'(\eta)\frac{2r}{a^2}c - 2\bar{k}\rho_\infty(cf')'$$
$$\frac{2r^2}{a^2}c - 2\bar{k}\rho_\infty cf' \Rightarrow \frac{1}{r}\frac{\partial}{\partial r}\left[r\frac{\partial(\rho u)}{\partial r}\right]$$
$$= -\frac{\bar{k}a^2}{r^3}\rho_\infty f - \frac{4\bar{k}r}{a^2}\rho_\infty c(cf')'$$

Then r-momentum is:

$$-\frac{\bar{k}a^2}{r}\frac{\rho_\infty}{\rho}f(\eta)\left[\frac{\bar{k}a^2}{r^2}\rho_\infty f(\eta)-2\bar{k}\rho_\infty cf'\right]-\frac{\bar{k}^2a^4}{r^3}\rho_\infty\frac{G^2}{c}$$

$$=-\rho_\infty\bar{k}^2a^2\frac{\partial p}{\partial\eta}\frac{2r}{a^2}c$$

$$+\upsilon\left[-\frac{\bar{k}a^2}{r^3}\rho_\infty f-\frac{4\bar{k}r}{a^2}\rho_\infty c(cf')'+\frac{\bar{k}a^2}{r^3}\rho_\infty f\right]$$

After omitting underlined phrases:

$$-\frac{\bar{k}^2a^4}{r^3}\frac{\rho_\infty}{\rho}\rho_\infty f^2+\frac{2\bar{k}^2a^2}{r}\frac{\rho_\infty}{\rho}\rho_\infty ff'-\frac{\bar{k}^2a^4}{r^3}\rho_\infty\frac{G^2}{c}$$

$$=-2\rho_\infty\bar{k}^2cr\frac{\partial p}{\partial\eta}-\frac{4\bar{k}\upsilon}{a^2}rc\rho_\infty(cf')'$$

Dividing by $2\bar{k}^2r\rho_\infty$ and using $r^2=a^2\Gamma(\eta)$,

$$-\frac{1}{2}\frac{a^4}{r^4}\frac{f^2}{c}+\frac{a^2}{r^2}\frac{ff'}{c}-\frac{a^4}{2r^4}\frac{G^2}{c}=$$

$$c(cf')'\longrightarrow r^2=a^2\Gamma(\eta)\frac{\partial p}{\partial\eta}=\frac{1}{2}\left(\frac{f}{\Gamma c}\right)^2$$

$$-\frac{ff'}{\Gamma c^2}+\frac{1}{2}\left(\frac{G}{\Gamma c}\right)^2-\frac{1}{Re}(cf')'$$

Integrating this, we have:

$$p-p_0=\int_0^\eta\left[\frac{1}{2}\left(\frac{f}{\Gamma c}\right)^2-\frac{ff'}{\Gamma c^2}+\frac{1}{2}\left(\frac{G}{\Gamma c}\right)^2-\frac{1}{Re}(cf')'\right]$$

$$\mathrm{d}\eta+c_1(Z)$$

Here, c_1 is a function of z which will be calculated by use of z-momentum as

$$u\frac{\partial(\rho w)}{\partial r}+w\frac{\partial(\rho w)}{\partial z}=-\frac{\partial P}{\partial z}$$

But at $r\to\infty:\rho w=2\bar{k}z\rho_\infty\Rightarrow$

$$\begin{cases}\dfrac{\partial(\rho w)}{\partial r}=0\\\dfrac{\partial(\rho w)}{\partial z}=2\bar{k}\rho_\infty\end{cases},\quad\frac{\partial P}{\partial z}=\rho_\infty\bar{k}^2a^2\frac{\partial p}{\partial z}.$$

Then:

$$-\rho_\infty\bar{k}^2a^2\frac{\mathrm{d}c_1(z)}{\mathrm{d}z}=2\bar{k}z(2\bar{k}\rho_\infty)\Rightarrow\frac{\mathrm{d}c_1(z)}{\mathrm{d}z}=-\frac{4z}{a^2}\Rightarrow c_1(z)$$

$$=-2\left(\frac{z}{a}\right)^2$$

This gives pressure as:

$$p-p_0=\int_0^\eta\left[\frac{1}{2}\left[\frac{f}{\Gamma c}\right]^2-\frac{ff'}{\Gamma c^2}+\frac{1}{2}\left(\frac{G}{\Gamma c}\right)^2-\frac{1}{Re}(cf')'\right]$$

$$\mathrm{d}\eta-2\left(\frac{z}{a}\right)^2$$

2. To derive (11):

Start from z-momentum:

$$u\frac{\partial(\rho w)}{\partial r}+w\frac{\partial(\rho w)}{\partial z}=-\frac{\partial P}{\partial z}$$

$$+\upsilon\left\{\frac{1}{r}\frac{\partial}{\partial r}\left[r\frac{\partial(\rho w)}{\partial r}\right]+\frac{\partial^2(\rho w)}{\partial z^2}\right\}$$

But:

$$\frac{\partial(\rho w)}{\partial r}=\frac{\partial(\rho w)}{\partial\eta}\frac{\partial\eta}{\partial r}=(2\bar{k}c'f'z+2\bar{k}cf''z)\rho_\infty\frac{2r}{a^2}c\Rightarrow r\frac{\partial(\rho w)}{\partial r}$$

$$=(2\bar{k}cc'f'z+2\bar{k}c^2f''z)\rho_\infty\frac{2r^2}{a^2}\Rightarrow\frac{\partial}{\partial r}\left[r\frac{\partial(\rho w)}{\partial r}\right]$$

$$=\left[2\bar{k}cc'f'z+2\bar{k}c^2f''z\right]\rho_\infty\frac{4r}{a^2}+\left[2\bar{k}(c')^2cf'z\right.$$

$$\left.+2\bar{k}c^2c''f'z+6\bar{k}c^2c'f''z.+2\bar{k}c^3f'''z\right]\rho_\infty\frac{4r^3}{a^4}$$

$$\Rightarrow\frac{1}{r}\frac{\partial}{\partial r}\left[r\frac{\partial(\rho w)}{\partial r}\right]$$

$$=\left[2\bar{k}cc'f'z+2\bar{k}c^2f''z\right]\rho_\infty\frac{4}{a^2}$$

$$+\left[2\bar{k}(c')^2cf'z+2\bar{k}c^2c''f'z+6\bar{k}c^2c'f''z\right.$$

$$\left.+2\bar{k}c^3f'''z\right]\rho_\infty\frac{4}{a^2}\Gamma(\eta)$$

Substitute in z-momentum:

$$-\frac{\bar{k}a^2}{r}\frac{\rho_\infty}{\rho}f(2\bar{k}c'f'z+2\bar{k}cf''z)\rho_\infty\frac{2r}{a^2}\frac{\rho}{\rho_\infty}+\frac{1}{\rho}(2\bar{k}\rho_\infty cf'z)$$

$$2\bar{k}\rho_\infty\frac{\rho}{\rho_\infty}f'=\upsilon\left\{\left[2Kcc'fz+2Kc^2f''z\right]\rho_\infty\frac{4}{a^2}\right.$$

$$+\left[2\bar{k}(c')^2cf'z+2\bar{k}c^2c''f'z+6\bar{k}c^2c'f''z\right.$$

$$\left.+2\bar{k}c^3f'''z\right]\rho_\infty\frac{4}{a^2}\Gamma(\eta)\left.\right\}-\rho_\infty\bar{k}^2a^2\left(-\frac{4z}{a^2}\right)$$

Equating the coefficient of z, the equation for f is:

$$-4\bar{k}^2c'ff'-4\bar{k}^2cff''+4\bar{k}^2c(f')^2$$

$$=\frac{8\bar{k}\upsilon}{a^2}cc'f'+\frac{8\bar{k}\upsilon}{a^2}c^2f''+\frac{8\bar{k}\upsilon}{a^2}(c')^2c\Gamma f'$$

$$+\frac{8\bar{k}\upsilon}{a^2}c^2c''\Gamma f'+\frac{24\bar{k}\upsilon}{a^2}c^2c'f''+\frac{8\bar{k}\upsilon}{a^2}c^3\Gamma f'''+4\bar{k}^2$$

3. To derive (12):

Start from φ-momentum:

$$u\frac{\partial(\rho v)}{\partial r}+\frac{\rho uv}{r}+w\frac{\partial(\rho v)}{\partial z}$$

$$=\upsilon\left\{\frac{1}{r}\frac{\partial}{\partial r}\left[r\frac{\partial(\rho v)}{\partial r}\right]-\frac{(\rho v)}{r^2}+\frac{\partial^2(\rho v)}{\partial z^2}\right\}$$

But:

$$\frac{\partial\left(\rho\,v\right)}{\partial r} = -\bar{k}\frac{a^2}{r^2}\rho_\infty G(\eta) + \bar{k}\frac{a^2}{r}\rho_\infty G'(\eta)\frac{2r}{a^2}C(\eta)$$

And

$$\frac{1}{r}\frac{\partial}{\partial r}\left[r\frac{\partial(\rho v)}{\partial r}\right] = \frac{\bar{k}a^2}{r^3}\rho_\infty G(\eta) + \frac{4\bar{k}r}{a^2}\rho_\infty cc'G'$$
$$+ \frac{4\bar{k}r}{a^2}\rho_\infty c^2 G''$$

Then $\boldsymbol{\varphi}$-momentum is:

$$-\frac{\bar{k}a^2}{r}\frac{f}{c}\left(-\frac{\bar{k}a^2}{r^2}\rho_\infty G + 2\bar{k}\rho_\infty cG'\right) + \frac{1}{r}\left(-\frac{\bar{k}a^2}{r}\rho_\infty f\frac{\bar{k}a^2}{r}\frac{G}{c}\right)$$
$$= \upsilon\left(\frac{\bar{k}a^2}{r^3}\rho_\infty G + \frac{4\bar{k}r}{a^2}\rho_\infty cc'G' + \frac{4\bar{k}r}{a^2}\rho_\infty c^2 G'' - \frac{\bar{k}a^2}{r^3}\rho_\infty G\right)$$

After omitting underlined phrases and dividing by $\frac{4\bar{k}\upsilon\rho_\infty}{r}$:

$$-\frac{\bar{k}a^2}{2\,\upsilon}f\,G' = \frac{r^2}{a^2}cc'G' + \frac{r^2}{a^2}c^2 G''$$

To derive energy equation, Eq. (17):

Consider a change in variable as: $\frac{T(\eta)-T_\infty}{T_w - T_\infty} = \theta(\eta)$ or $\theta(\eta) = \frac{T(\eta)-T_\infty}{\frac{a\,q_w}{2k}}$. Then energy equation can be written as:

$$\rho\,u\frac{\partial\theta}{\partial r} + \rho\,w\frac{\partial\theta}{\partial z} = \frac{\mu}{Pr}\frac{1}{r}\frac{\partial}{\partial r}\left(r\frac{\partial\theta}{\partial r}\right)$$

Using chain rule:

$$\frac{\partial\theta}{\partial r} = \frac{\partial\theta}{\partial\eta}\frac{\partial\eta}{\partial r} = \frac{2r}{a^2}c\theta', \quad \frac{\partial\theta}{\partial z} = 0$$

$$r\frac{\partial\theta}{\partial r} = \frac{2r^2}{a^2}c\theta' \Rightarrow \frac{\partial}{\partial r}\left(r\frac{\partial\theta}{\partial r}\right)$$

$$= \frac{4r}{a^2}c\theta' + (c'\theta' + c\theta'')\frac{4r^3}{a^4}c \Rightarrow \frac{1}{r}\left[\frac{\partial}{\partial r}\left(r\frac{\partial\theta}{\partial r}\right)\right]$$

$$= \frac{4}{a^2}c\theta' + (c'\theta' + c\theta'')\frac{4r^2}{a^4}c \longrightarrow r^2 = a^2\Gamma(\eta)\frac{1}{r}$$

$$\left[\frac{\partial}{\partial r}\left(r\frac{\partial\theta}{\partial r}\right)\right]$$

$$= \frac{4}{a^2}c\theta' + \frac{4\Gamma}{a^2}c(c'\theta' + c\theta'')$$

By substitution:

$$-\frac{\bar{k}a^2}{r}\rho_\infty f\frac{2r}{a^2}\frac{\rho}{\rho_\infty}\theta' = \frac{\mu}{Pr}\frac{4}{a^2}\left(c\theta' + \Gamma cc'\theta' + \Gamma c^2\theta''\right)$$

Divide by $2\bar{k}\rho$ and since, $1/Re = 2v/\bar{k}a^2$

$$\frac{1}{Re\cdot Pr}\left(c^2\Gamma\theta'' + \Gamma cc'\theta' + c\theta'\right) + f\theta' = 0$$

References

Abbasi AS, Rahimi AB (2009a) Non-axisymmetric three-dimensional stagnation-point flow and heat transfer on a flat plate. J Fluids Eng 131(7):074501.1–074501.5

Abbasi AS, Rahimi AB (2009b) Three-dimensional stagnation-point flow and heat transfer on a flat plate with transpiration. J Thermophys Heat Transfer 23(3):513–521

Abbasi AS, Rahimi AB (2012) Investigation of two-dimensional stagnation-point flow and heat transfer impinging on a flat plate. J Heat Transf Tech Brief 134(6):064501

Abbasi AS, Rahimi AB, Niazman H (2011) Exact solution of three-dimensional unsteady stagnation flow on a heated plate. J Thermodyn Heat Transf 25(1):55–58

Afzal N, Ahmad S (1975) Effect of suction and injection on self-similar solutions of second-order boundary layer equations. Int J Heat Mass Transf 18:607–614

Chamkha AJ (2000) Flow of two-immiscible fluids in porous and nonporous channels. J Fluids Eng 122(1):117–124

Chamkha AJ, Ahmed SE (2011) Similarity solution for unsteady MHD flow near a stagnation point of a three-dimensional porous body with heat and mass transfer, heat generation/absorption and chemical reaction. J Appl Fluid Mech 4(1):87–94

Chamkha AJ, Khaled AA (2000) Similarity solutions for hydromagnetic mixed convection heat and mass transfer for Hiemenz flow through porous media. Int J Numer Meth Heat Fluid Flow 10(1):94–115

Cunning GM, Davis AMJ, Weidman PD (1998) Radial stagnation flow on a rotating cylinder with uniform transpiration. J Eng Math 33:113–128

Davey A (1951) Boundary layer flow at a Saddle point of attachment. J Fluid Mech 10:593–610

Gersten K, Papenfuss HD, Gross JF (1978) Influence of the Prandtl number on second-order heat transfer due to surface curvature at a three-dimensional stagnation point. Int J Heat Mass Transf 21:275–284

Gorla RSR (1976) Heat transfer in an axisymmetric stagnation flow on a cylinder. Appl Sci Res 32:541–553

Gorla RSR (1977) Unsteady laminar axisymmetric stagnation flow over a circular cylinder. Dev Mech 9:286–288

Gorla RSR (1978a) Nonsimilar axisymmetric stagnation flow on a moving cylinder. Int J Sci 16:392–400

Gorla RSR (1978b) Transient response behavior of an axisymmetric stagnation flow on a circular cylinder due to time-dependent free stream velocity. Lett Appl Eng Sci 16:493–502

Gorla RSR (1979) Unsteady viscous flow in the vicinity of an axisymmetric stagnation-point on a cylinder. Int. Sci. 17:87–93

Grosch CE, Salwen H (1982) Oscillating stagnation-point flow. Proc R Soc Lond A384:175–190

Hiemenz K (1911) Die grenzchicht an einem in den gleichformingen Flussigkeitsstrom eingetauchten geraden KreisZylinder. Dinglers Polytech J 326:321–410

Homann FZ (1936) Der EINFLUSS GROSSER Zahighkeit bei der Strmung um den Zylinder und um die Kugel. Z Angew Math Mech 16:153–164

Hong L, Wang CY (2009) Annular axisymmetric stagnation flow on a moving cylinder. Int J Eng Sci 47:141–152

Howarth L (1951) The boundary layer in three-dimensional flow. Part II. The flow near stagnation point. Philos Mag 42:1433–1440

Katz A (1972) Transformations of the compressible boundary layer equations. SIAM J Allied Math 22(4):604–611

Kumari M, Nath G (1980) Unsteady compressible 3-dimensional boundary layer flow near an axisymmetric stagnation point with mass transfer. Int J Eng Sci 18:1285–1300

Kumari M, Nath G (1981) Self-similar solution of unsteady compressible three-dimensional stagnation-point boundary layers. J Appl Math Phys 32:267–276

Libby PA (1967) Heat and mass transfer at a general three-dimensional stagnation point. AIAA J 5(3):507–517

Magyari E, Chamkha AJ (2008) Exact analytical results for the thermosolutal MHD Marangoni boundary layers. Int J Therm Sci 47(7):848–857

Mohammadiun H, Rahimi AB (2012) Stagnation-point flow and heat transfer of a viscous, compressible fluid on a cylinder. J Thermophys Heat Transfer 26(3):494–502

Mohammadiun H, Rahimi AB, Kianifar A (2013) Axisymmetric stagnation-point flow and heat transfer of a viscous, compressible fluid on a cylinder with constant heat flux. Sci Iran B 20(1):185–194

Mudhaf AA, Chamkha AJ (2005) Similarity solutions for MHD thermosolutal Marangoni convection over a flat surface in the presence of heat generation or absorption effects. Heat Mass Transf 42:112–121

Press WH, Flannery BP, Teukolsky SA, Vetterling WT (1997) Numerical recipes, the art of scientific computing. Cambridge University Press, Cambridge

Rahimi AB, Saleh R (2007) Axisymmetric stagnation-point flow and heat transfer of a viscous fluid on a rotating cylinder with time-dependent angular velocity and uniform transpiration. J Fluids Eng 129:107–115

Rahimi AB, Saleh R (2008) Similarity solution of unaxisymmetric heat transfer in stagnation-point flow on a cylinder with simultaneous axial and rotational movements. J Heat Transf Tech Brief 130:054502-1–054502-5

Rahimi AB, Mohammadiun H, Mohammadiun M (2016) Axisymmetric stagnation flow and heat transfer of a compressible fluid impinging on a cylinder moving axially. ASME J Heat Transf 138(2):022201

Saleh R, Rahimi AB (2004) Axisymmetric stagnation-point flow and heat transfer of a viscous fluid on a moving cylinder with time-dependent axial velocity and uniform transpiration. J Fluids Eng 126:997–1005

Subhashini SV, Nath G (1999) Unsteady compressible flow in the stagnation region of two-dimensional and axisymmetric bodies. Acta Mech 134:135–145

Takhar HS, Chamkha AJ, Nath J (1999) Unsteady axisymmetric stagnation-point flow of a viscous fluid on a cylinder. Int J Eng Sci 37:1943–1957

Takhar HS, Chamkha AJ, Nath G (2000) Combined heat and mass transfer along a vertical moving cylinder with a free stream. Heat Mass Transf 36:237–246

Takhar HS, Chamkha AJ, Nath G (2001) Unsteady three-dimensional MHD-boundary-layer flow due to the impulsive motion of a stretching surface. Acta Mech 146(1):59–71

Takhar HS, Chamkha AJ, Nath G (2002) Natural convection on a vertical cylinder embedded in a thermally stratified high-porosity medium. Int J Therm Sci 41(1):83–93

Umavathi JC, Chamkha AJ (2005) Unsteady two-fluid flow and heat transfer in a horizontal channel. Heat Mass Transf 42:81–90

Wang CY (1973) Axisymmetric stagnation flow towards a moving plate. Am Inst Chem Eng J 19(5):1080–1082

Wang CY (1974) Axisymmetric stagnation flow on a cylinder. Q Appl Math 32:207–213